A GENERAL GEOMETRIC MODEL FOR CASTING DIFFRACTION

JOEL VINCENT BERNIER

ABSTRACT. A complete and general geometric model for describing diffraction measurements is presented. It includes provisions for describing both mono- and poly-chromatic schemas for *collimated* incident beams (*i.e.* negligable beam divergence). Detectors are modeled as planar bodies, and their shapes and placements in the reference frame are completely arbitrary. The mapping that takes an admissable reciprocal lattice vector in the crystal frame to pixel coordinates in a given detector frame is of the form $\mathbf{A}(\mathbf{x}) \cdot \mathbf{x} = \mathbf{y}$. The application of focus in this note is the rotation method; this implies a monochromatic incident beam and a sample frame that rotates about an axis that is nominally perpendicular to the incident beam, with provision for finite deviations.

1. COORDINATE SYSTEMS

A single-detector diffraction measurement schema is illustrated in Figure 1. For genearlity we utilize five fundamental coordinate systems:

- the **laboratory** frame, $\left\{ \hat{\mathbf{X}}_l \hat{\mathbf{Y}}_l \hat{\mathbf{Z}}_l \right\}$;
- the **beam** frame, $\left\{ \hat{\mathbf{X}}_b \hat{\mathbf{Y}}_b \hat{\mathbf{Z}}_b \right\}$;
- the **detector** frame(s), $\left\{ \hat{\mathbf{X}}_d \hat{\mathbf{Y}}_d \hat{\mathbf{Z}}_d \right\}_i$;
- the **sample** frame, $\left\{ \hat{\mathbf{X}}_s \hat{\mathbf{Y}}_s \hat{\mathbf{Z}}_s \right\}$; and
- the **crystal** frame, $\left\{ \hat{\mathbf{X}}_c \hat{\mathbf{Y}}_c \hat{\mathbf{Z}}_c \right\}$.

1.1. **Laboratory Frame.** The laboratory frame is intended to provide a global reference frame that is stationary during the measurement. The incident beam has a non-neglible physical extent in the lab frame, typically possessing a rectangular or circular cross-section. The beam direction is represented by the unit vector $\hat{\mathbf{b}}$, and the centroid of its cross-section is defined to coincide with the origin of $\left\{\hat{\mathbf{X}}_l\hat{\mathbf{Y}}_l\hat{\mathbf{Z}}_l\right\}$, labeled P0.

1.2. **Beam Frame.** When working with diffraction geometry, it becomes very useful to associate detector-relative cartesian coordinates with a bragg angle, 2θ, and azimuth, η. In the present notation, the bragg angle (see Equation 16) is defined as

$$(1) \qquad\qquad 2\theta \equiv \arccos\left(\hat{\mathbf{b}} \cdot \hat{\mathbf{d}}\right)$$

where $\hat{\mathbf{d}}$ is the unit vector along the diffracted beam

$$(2) \qquad\qquad \hat{\mathbf{d}} \equiv \frac{\text{P4} - \text{P3}}{\|\text{P4} - \text{P3}\|}$$

and $\hat{\mathbf{b}}$ is the propagation direction of the incident beam, or the unit incident wavevector (see § 1.3, 1.5). Given the axisymmetry inherent in the definition of the diffraction condition, it also becomes useful to describe $\hat{\mathbf{d}}$ in terms of an azimuthal angle, η; this requires defining a reference azimuth, which is done using a vector $\hat{\mathbf{e}}$ perpendicular to $\hat{\mathbf{b}}$. In terms of $\hat{\mathbf{e}}$, $\hat{\mathbf{b}}$, and $\hat{\mathbf{d}}$

$$(3) \qquad\qquad \eta = \arccos\left(\hat{\mathbf{e}} \cdot \left(\mathbf{I} - \hat{\mathbf{b}} \otimes \hat{\mathbf{b}}\right) \cdot \hat{\mathbf{d}}\right).$$

One benefit of the beam frame is that the components of a unit reciprocal lattice vector, $\hat{\mathbf{G}}$, satisfying the bragg condition can be written exclusively in terms of 2θ and η

$$
(4) \qquad \left[\hat{\mathbf{G}}\right]_b = \begin{Bmatrix} \cos\eta\cos\theta \\ \sin\eta\cos\theta \\ \sin\theta \end{Bmatrix}
$$

The change of basis matrix taking components in $\left\{\hat{\mathbf{X}}_b\hat{\mathbf{Y}}_b\hat{\mathbf{Z}}_b\right\}$ to $\left\{\hat{\mathbf{X}}_l\hat{\mathbf{Y}}_l\hat{\mathbf{Z}}_l\right\}$ is defined as

$$
(5) \qquad \mathsf{r}_b = \left[\hat{\mathbf{e}}, \ -\hat{\mathbf{b}}\times\hat{\mathbf{e}}, \ -\hat{\mathbf{b}}\right].
$$

1.3. **Detector Frame.** A typical detector element has a planar active area with a rectangular shape. A complete instrument may contain several independent detectors with unique orientations and placements in the lab frame. A cartesian coordinate system $\left\{\hat{\mathbf{X}}_d\hat{\mathbf{Y}}_d\hat{\mathbf{Z}}_d\right\}$ is attached to each independent detector element as follows: the origin P1 is coincident with the centroid of the active surface, and $\hat{\mathbf{Z}}_d$ represents the plane normal. The $\hat{\mathbf{X}}_d, \hat{\mathbf{Y}}_d$ directions are typically aligned with the horizontal and vertical pixel-relative directions on each panel. The coordinates of points in each independent detector coordinate system, $\left\{\hat{\mathbf{X}}_d\hat{\mathbf{Y}}_d\hat{\mathbf{Z}}_d\right\}$ are related to coordinated in $\left\{\hat{\mathbf{X}}_l\hat{\mathbf{Y}}_l\hat{\mathbf{Z}}_l\right\}$ via a simple affine transformation:

$$
(6) \qquad [\mathbf{x}]_l = \mathsf{R}_d \cdot [\mathbf{x}]_d + [\mathbf{t}_d]_l
$$

where $\mathbf{t}_d = \mathrm{P1} - \mathrm{P0}$ and the notation $[\mathbf{x}]_l$ indicates the components of $\mathbf{x}$ in $\left\{\hat{\mathbf{X}}_l\hat{\mathbf{Y}}_l\hat{\mathbf{Z}}_l\right\}$. Because only planar detectors are considered, the components of a detector-relative point are of the form $[\mathbf{x}]_d = [x \ y \ 0]$.

1.4. **Sample Frame.** The sample frame provides a basis in which to represent a uniquely oriented and located specimen. For the arbitrarily defined sample-relative vector $\mathbf{S}$, coordinates in $\left\{\hat{\mathbf{X}}_s\hat{\mathbf{Y}}_s\hat{\mathbf{Z}}_s\right\}$ are connected to $\left\{\hat{\mathbf{X}}_l\hat{\mathbf{Y}}_l\hat{\mathbf{Z}}_l\right\}$ via the affine transformation

$$(7) \qquad\qquad [\mathbf{s}]_l = \mathsf{R}_s \cdot [\mathbf{s}]_s + [\mathbf{t}_s]_l$$

where $\mathbf{t}_s = \mathrm{P2} - \mathrm{P0}$. In the case of the rotation method, this is frame is the oscillation frame. Without loss of generality, the oscillation axis is fixed to $\hat{\mathbf{Y}}_s$. It may be canted with respect to $\hat{\mathbf{Y}}_l$ by the angle χ[1]. The oscillation angle itself is represented by ω. The full model has a sufficient number of degrees of freedom to preclude the need for a third rotational degree of freedom for $\left\{\hat{\mathbf{X}}_s\hat{\mathbf{Y}}_s\hat{\mathbf{Z}}_s\right\}$.

1.5. **Crystal Frame.** The crystal frame represent a local RHON coordinate system attached to the lattice of a single-crystal domain in the sample. In the context of far-field HEDM, the origin of $\left\{\hat{\mathbf{X}}_c\hat{\mathbf{Y}}_c\hat{\mathbf{Z}}_c\right\}$, labeled P3, represents the centroid of the crystallite. For a crystal-relative vector $\mathbf{c}$, the components are transformed as

$$(8) \qquad\qquad [\mathbf{c}]_s = \mathsf{R}_c \cdot [\mathbf{c}]_c + [\mathbf{t}_c]_s$$

$$(9) \qquad\qquad [\mathbf{c}]_l = \mathsf{R}_s \cdot \mathsf{R}_c \cdot [\mathbf{c}]_c + \mathsf{R}_s \cdot [\mathbf{t}_c]_s + [\mathbf{t}_s]_l$$

where $\mathbf{t}_c = \mathrm{P3} - \mathrm{P2}$. The forumaltion of diffracted beam vectors for a given unit cell is discussed in § 2.

---

[1]the canting angle χ is typically very small for an HEDM schema, although some special cases might require it to be set to some non-zero value. Including this degree of freedom in the model also allows for it to be quantified via calibration.
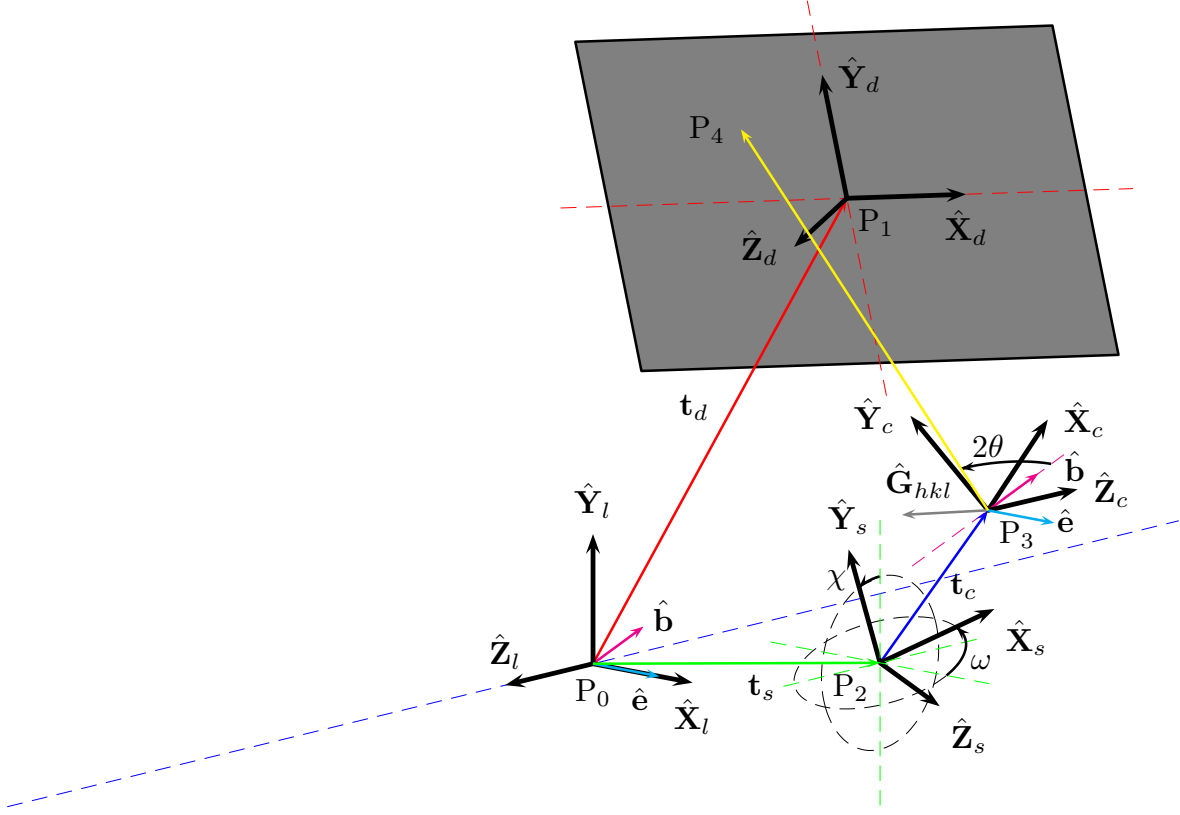
FIGURE 1. A single-detector diffraction schema illustrating the four funda-
mental coordinate systems and the 5 generic points P0-P4 used to cread
the transfer function taking reciprocal lattice vector components to detector-
relative components. For completeness, the reciprocal lattice vector **G** and
bragg angle 2θ associated with P4 are shown. The azimuthal angle, η, of $\hat{\mathbf{G}}$
about $\hat{\mathbf{b}}$ is not shown; however, the reference azimuth is, denoted by the unit
vector $\hat{\mathbf{e}}$.

2. DIFFRACTION

2.1. **Convention for writing components of crystal lattice vectors.** In order to
insert the geometry of diffraction into the coordinate system hierarchy described above, it
is necessary to etablish a convention for describing the crystal lattice. The crystal lattice
itself may be parameterized by its primitive vectors **a**, **b**, and **c**. They share a common

origin at a lattice site and are subject to the following conditions:

$$
\begin{aligned}
\|\mathbf{a}\| &= a \\
\|\mathbf{b}\| &= b \\
\|\mathbf{c}\| &= c \\
\tfrac{1}{bc}\mathbf{b}\cdot\mathbf{c} &= \cos\alpha \\
\tfrac{1}{ca}\mathbf{c}\cdot\mathbf{a} &= \cos\beta \\
\tfrac{1}{ab}\mathbf{a}\cdot\mathbf{b} &= \cos\gamma
\end{aligned}
\tag{10}
$$

The six scalar cell parameters $\{a, b, c, \alpha, \beta, \gamma\}$ represent a convenient parameterization of the reference unit cell, which typically correspond to an unloaded state at a reference temperature. Crystal symmetry operations (excluding triclinic) generate equivalences among cell parameters; however once a crystal is deformed, the reference symmetry is broken and all six parameters must be considered as independent. The treatment of strained crystals in the context of the reference crystal symmetry is discussed in detail below. For writing components of crystal-relative vectors and tensors in $\left\{\hat{\mathbf{X}}_c\hat{\mathbf{Y}}_c\hat{\mathbf{Z}}_c\right\}$, a convention must be chosen to register the lattice vectors. The convention employed herein is consistent with that proposed by [3]. Explicitly stated, $\mathbf{a} \parallel \hat{\mathbf{X}}_c$ and $(\mathbf{a} \times \mathbf{b}) \parallel \hat{\mathbf{Z}}_c$, as depicted in Figure 2.

The reciprocal lattice, which forms a dual basis to the direct lattice, is a very useful concept in diffraction. The reciprocal lattice vectors are defined[2] as follows:

$$
\mathbf{a}^* = \frac{1}{v}\mathbf{b} \times \mathbf{c}
\tag{11}
$$

$$
\mathbf{b}^* = \frac{1}{v}\mathbf{c} \times \mathbf{a}
\tag{12}
$$

$$
\mathbf{c}^* = \frac{1}{v}\mathbf{a} \times \mathbf{b}
\tag{13}
$$

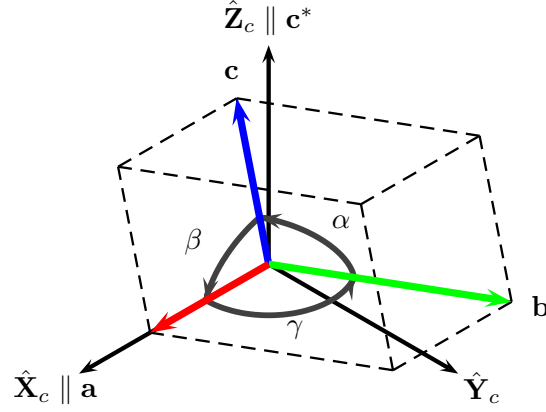[2]this is the so-called "crystallographer's convention" where the prefactor of 2π is omitted.

FIGURE 2. The convention for describing the reference (read: unstrained) lattice has $\mathbf{a} \parallel \hat{\mathbf{X}}_c$ and $\mathbf{c}^* \parallel \hat{\mathbf{Z}}_c$. Note that a triclinic primitive cell is depicted for generality. The crystal orientation, R_c, takes components in the crystal frame, $\left\{ \hat{\mathbf{X}}_c \hat{\mathbf{Y}}_c \hat{\mathbf{Z}}_c \right\}$, to the sample frame, $\left\{ \hat{\mathbf{X}}_s \hat{\mathbf{Y}}_s \hat{\mathbf{Z}}_s \right\}$.

where $v = \mathbf{a} \cdot \mathbf{b} \times \mathbf{c}$ represents the volume of the primitive cell. The change-of-basis matrix, B, that takes vector components in the reciprocal lattice frame to the crystal frame is formulated as

$$(14) \qquad \mathsf{B} = \begin{bmatrix} \mathbf{a}^* & \mathbf{b}^* & \mathbf{c}^* \end{bmatrix}_c$$

$$= \frac{1}{v} \begin{bmatrix} bc\sin\alpha^*\sin\beta\sin\gamma & 0 & 0 \\ -bc\sin\alpha^*\sin\beta\cos\gamma & ac\sin\alpha^*\sin\beta & 0 \\ -bc(\cos\alpha^*\sin\beta\cos\gamma + \cos\beta\sin\gamma) & ac\cos\alpha^*\sin\beta & ab\sin\gamma \end{bmatrix},$$

where $\{a^*, b^*, c^*, \alpha^*, \beta^*, \gamma^*\}$ are the reciprocal lattice parameters defined analogously to the direct lattice parameters in Figure 2 and Equation 10.

Assume that a reciprocal lattice vector, $\mathbf{G}$, satisfies a bragg condition. The unit vector aligned with its associated diffracted beam, $\hat{\mathbf{d}}$, is then

$$\hat{\mathbf{d}} = \mathsf{R}\left(\pi, \hat{\mathbf{G}}\right) \cdot \left(-\hat{\mathbf{b}}\right)$$

$$= \left(2\hat{\mathbf{G}} \otimes \hat{\mathbf{G}} - \mathbf{I}\right) \cdot \left(-\hat{\mathbf{b}}\right)$$

$$\tag{15} = \left(\mathbf{I} - 2\hat{\mathbf{G}} \otimes \hat{\mathbf{G}}\right) \cdot \hat{\mathbf{b}}$$

$$\tag{16} \text{where } \hat{\mathbf{G}} \cdot \hat{\mathbf{b}} = -\frac{\lambda}{2}\|\mathbf{G}\| = -\sin\theta,$$

$$\tag{17} \hat{\mathbf{d}} \cdot \hat{\mathbf{Z}}_d < 0,$$

$\hat{\mathbf{G}} = \mathbf{G}/\|\mathbf{G}\|$, and $\hat{\mathbf{b}}$ is the unit vector aligned with the beam propagation direction. Equation 16 is the bragg condition for X-rays having wavelength λ, and Equation 17 is the geometric condition ensuring that $\hat{\mathbf{d}}$ can intersect the detector plane. Note that there is an additional condition that must be satisfied in the instrument for P4 to be observable; it must also lie within the physical extent of the detector element. Application of this condition is, however, quite straightforward and not explicitly stated in this document.

2.2. **Representing crystal orientation and strain.** A reciprocal lattice vector, $\mathbf{G}$, is typically representend by its components in the reference (read: undistorted) reciprocal lattice frame, $[\mathbf{G}]_* = [h\ k\ l]$. The change-of-basis matrix, B, that takes components in the reciprocal lattice to $\left\{\hat{\mathbf{X}}_c\hat{\mathbf{Y}}_c\hat{\mathbf{Z}}_c\right\}$ was given by Equation 14 above (§ 2.1). The effects of both finite distortion and rotation of a crystal lattice with respect to $\left\{\hat{\mathbf{X}}_s\hat{\mathbf{Y}}_s\hat{\mathbf{Z}}_s\right\}$ are captured using a deformation gradient tensor, $\mathbf{F}$, as presented in [1]. The tensor $\mathbf{F}$ acts on the *direct* lattice vectors, and takes undistorted lattice vectors in the reference crystal frame, $\left\{\hat{\mathbf{X}}_c\hat{\mathbf{Y}}_c\hat{\mathbf{Z}}_c\right\}$, to reoriented and distorted lattice vectors in the sample frame,

$\left\{\hat{\mathbf{X}}_s\hat{\mathbf{Y}}_s\hat{\mathbf{Z}}_s\right\}$. Using the polar decomposition,

(18) $$\mathbf{F} = \mathsf{V}\mathsf{R}_c, \ \forall \ \mathbf{V} \in Sym^{3\times3}, \ \mathsf{R}_c \in SO^3,$$

where R_c is the crystal orientation and $\mathbf{V}$ is the "left" stretch tensor. Edmiston et al. [2] have shown that $\mathbf{F}^{-T} = \mathbf{V}^{-1}\mathsf{R}_c$ can be applied analogously to reciprocal lattice vector components written in $\left\{\hat{\mathbf{X}}_c\hat{\mathbf{Y}}_c\hat{\mathbf{Z}}_c\right\}$. Given the reciprocal lattice vector $\mathbf{G}$, with components $[\mathbf{G}]_* = [h\ k\ l]$ in the reciprocal lattice frame, the fully distorted and orientend components in $\left\{\hat{\mathbf{X}}_l\hat{\mathbf{Y}}_l\hat{\mathbf{Z}}_l\right\}$ are then derived as

$$[\mathbf{G}]_l = \mathsf{R}_s\,[\mathbf{G}]_s$$

$$= \mathsf{R}_s\,\left[\mathbf{F}^{-T}\right]_s\,[\mathbf{G}]_c$$

$$= \mathsf{R}_s\,\left[\mathbf{F}^{-T}\right]_s\,\mathsf{B}\,[\mathbf{G}]_*$$

(19) $$\boxed{= \mathsf{R}_s\,\left[\mathbf{V}^{-1}\right]_s\,\mathsf{R}_c\mathsf{B}\,[\mathbf{G}]_*},$$

The three crystal orientation degrees of freedom are wrapped up in R_c, while the six that represent strain are contained in $\mathbf{V}$.

Functionally, the orientation degrees of freedom can be decoupled from the strain (and position) degrees of freedom in the initial analysis. This "orientation indexing" procedure essentially consists of testing discrete orientations $\mathsf{R}(\phi, \boldsymbol{n})$, for a set of feasible $\mathbf{G}$ and checking for intensity at the associated detector points P4. For the rotation method, the oscillation angle ω must be calculated for each feasible $\mathbf{G}$ as well; this will be discussed in § 4.

3. Parametric ray-plane intersection and the transform function

The coordinates of the points P0 − P4 (see Figure 1) in the lab frame are

$$(20) \qquad [\text{P0}]_l \equiv \begin{bmatrix} 0 & 0 & 0 \end{bmatrix}$$

$$(21) \qquad [\text{P1}]_l = [\mathbf{t}_d]_l$$

$$(22) \qquad [\text{P2}]_l = [\mathbf{t}_s]_l$$

$$(23) \qquad [\text{P3}]_l = \mathsf{R}_s \, [\mathbf{t}_c]_s + [\mathbf{t}_s]_l$$

$$(24) \qquad [\text{P4}]_l = \mathsf{R}_d \, [\mathbf{x}]_d + [\mathbf{t}_d]_l$$

Using the parametric equations for a plane (Equation 25) and line (Equation 26), we may obtain a system of equations linking $\hat{\mathbf{d}}$ and P4.

$$(25) \qquad \hat{\mathbf{Z}}_d \cdot (\text{P4} - \text{P1}) = 0$$

$$(26) \qquad \text{P4} = \text{P3} + u\hat{\mathbf{d}}$$

Substituting for P4 and rearranging to solve for the scale parameter u yields

$$\hat{\mathbf{Z}}_d \cdot (\text{P3} - \text{P1} + u\hat{\mathbf{d}}) = 0$$

$$\hat{\mathbf{Z}}_d \cdot (\text{P3} - \text{P1}) = -u\hat{\mathbf{Z}}_d \cdot \hat{\mathbf{d}}$$

$$(27) \qquad \implies u = \frac{\hat{\mathbf{Z}}_d \cdot (\text{P1} - \text{P3})}{\hat{\mathbf{Z}}_d \cdot \hat{\mathbf{d}}}$$

Finally, inserting this result into Equation 26 with some rearrangement yields

$$(28) \qquad \boxed{[\text{P4}]_d = \mathsf{R}_d^T \cdot \left[[\text{P3} - \text{P1}]_l - \frac{\text{dot}\left(\left[\hat{\mathbf{Z}}_d\right]_l^T, \ [\text{P3} - \text{P1}]_l \right)}{\text{dot}\left(\left[\hat{\mathbf{z}}_d\right]_l^T, \ \left[\hat{\mathbf{d}}\right]_l \right)} \left[\hat{\mathbf{d}}\right]_l \right]},$$

where $\left[\hat{\mathbf{d}}\right]_l$ is obtained from Equation 15 and Equation 19.

4. Solving for the oscillation angle, ω

For a monochromatic schema using the rotation method, the action of the oscillation in a canted configuration is represented by the rotation R_s where

$$
(29) \qquad \mathsf{R}_s = \mathsf{R}\left(\chi,\ \hat{\mathbf{X}}_l\right) \mathsf{R}\left(\omega,\ \hat{\mathbf{Y}}_l\right)
$$

$$
= \begin{bmatrix} 1 & 0 & 0 \\ 0 & \cos\chi & -\sin\chi \\ 0 & \sin\chi & \cos\chi \end{bmatrix} \begin{bmatrix} \cos\omega & 0 & \sin\omega \\ 0 & 1 & 0 \\ -\sin\omega & 0 & \cos\omega \end{bmatrix}
$$

$$
= \begin{bmatrix} \cos\omega & 0 & \sin\omega \\ \sin\chi\sin\omega & \cos\chi & -\sin\chi\cos\omega \\ -\cos\chi\sin\omega & \sin\chi & \cos\chi\cos\omega \end{bmatrix}.
$$

From Equation 19 we have

$$
(30) \qquad\qquad [\mathbf{G}]_s = \left[\mathbf{F}^{-T}\right]_s \mathsf{B}\,[\mathbf{G}]_*
$$

By writing the bragg condition (Equation 16) in terms of lab-frame components by multiplying by the normalized components $\left[\hat{\mathbf{G}}\right]_s$ above by R_s leads to relation of the form

$$
(31) \qquad\qquad a\sin\omega + b\cos\omega = c
$$

$$
(32) \qquad\qquad \equiv R\sin\left(x + \alpha\right)
$$

$$
(33) \qquad\qquad \text{where } R \equiv \sqrt{a^2 + b^2}, \text{ and } \alpha \equiv \operatorname{atan2}(b, a),
$$

and

$$(34) \qquad a = \left[\hat{G}_2\right]_s \left[\hat{b}_0\right]_l + \sin\chi \left[\hat{G}_0\right]_s \left[\hat{b}_1\right]_l - \cos\chi \left[\hat{G}_0\right]_s \left[\hat{b}_2\right]_l$$

$$(35) \qquad b = \left[\hat{G}_0\right]_s \left[\hat{b}_0\right]_l - \sin\chi \left[\hat{G}_2\right]_s \left[\hat{b}_1\right]_l + \cos\chi \left[\hat{G}_2\right]_s \left[\hat{b}_2\right]_l$$

$$(36) \qquad c = -\sin\theta - \cos\chi \left[\hat{G}_1\right]_s \left[\hat{b}_1\right]_l - \sin\chi \left[\hat{G}_1\right]_s \left[\hat{b}_2\right]_l$$

These yield the solutions

$$(37) \qquad \omega = \begin{cases} \arcsin\left(\frac{c}{\sqrt{a^2+b^2}}\right) - \alpha \\ \pi - \arcsin\left(\frac{c}{\sqrt{a^2+b^2}}\right) - \alpha \end{cases}$$

which are either unique (both sides of the diffraction cone), a double root (tangent to the diffraction cone – typically not considered) or do not exist ($|\frac{c}{\sqrt{a^2+b^2}}| > 1$, can't intersect diffraction cone).

5. Summary

The complete procedure for finding the detector coordinates of all reflections for a specifically oriented, strained crystal at the the position P3 consists of the following procedure:

(1) Generate $[h\ k\ l]$ up to the relevant order (determined by geometry and wavelength of the X-rays)

(2) Calculate the set of reciprocal lattice vector components in $\left\{\hat{\mathbf{X}}_s \hat{\mathbf{Y}}_s \hat{\mathbf{Z}}_s\right\}$ using Equation 30

(3) Calculate the set of oscillation angles, $(\omega_0,\ \omega_1)$, for each unique $[h\ k\ l]$ using Equation 37

(4) Calculate the set of unit diffraction vector components in $\left\{ \hat{\mathbf{X}}_l \hat{\mathbf{Y}}_l \hat{\mathbf{Z}}_l \right\}$ using Equation 29, Equation 19, Equation 15 for each valid oscillation angle pair in $(\omega_0, \ \omega_1)$

(5) Calculate $[\mathrm{P4}]_d$ from Equation 28.

References

[1] J. V. Bernier, N. R. Barton, U. Lienert, and M. P. Miller. Far-field high-energy diffraction microscopy: a tool for intergranular orientation and strain analysis. *The Journal of Strain Analysis for Engineering Design*, 46(7):527–547, July 2011. ISSN 0309-3247. doi: 10.1177/0309324711405761. URL http://sdj.sagepub.com/lookup/doi/10.1177/0309324711405761.

[2] J. K. Edmiston, J. V. Bernier, N. R. Barton, and G. C. Johnson. Lattice refinement strategies. *Acta crystallographica. Section A, Foundations of crystallography*, 68(Pt 2): 181–7, Mar. 2012. ISSN 1600-5724. doi: 10.1107/S010876731105598X. URL http://www.ncbi.nlm.nih.gov/pubmed/22338653.

[3] J. F. Nye. *Physical Properties of Crystals: Their Representation by Tensors and Matrices*, pages 276–288. Oxford University Press, 1985. URL http://www.oup.com/us/catalog/general/subject/EarthSciences/Geology/?view=usa&ci=9780198511656#Product_Details. Appendix B.